Journal of Catalysis **187,** 85–94 (1999)
Article ID jcat.1999.2565, available online at http://www.idealibrary.com on IDEAL®

Carbon and Oxygen Reaction Pathways of CO_2 Reforming of Methane over Ni/La_2O_3 and Ni/Al_2O_3 Catalysts Studied by Isotopic Tracing Techniques

V. A. Tsipouriari and X. E. Verykios

Department of Chemical Engineering, University of Patras, GR-26500 Patras, Greece

Received January 26, 1999; revised May 18, 1999; accepted May 18, 1999

Steady-state tracing techniques, using isotopically labeled molecules, were applied to study mechanistic aspects of the carbon and oxygen reaction pathways to form CO over Ni/La_2O_3 and Ni/Al_2O_3 catalysts. Over the Ni/La_2O_3 catalyst, it was found that under steady-state reaction conditions, the quantity of reversibly adsorbed CH_4 and the active carbon-containing intermediate species in the carbon pathway to form CO originating from CH_4 is higher than the respective quantities derived from the CO_2 molecule. Over the Ni/Al_2O_3 catalyst, much smaller quantities of reversibly adsorbed CH_4 and active carbon-containing species, originated from the CH_4 molecule, which lead to CO formation were detected. It was also determined that a large quantity of oxygen atoms, originating from the La_2O_3 support of the Ni/La_2O_3 catalyst, participate in the reaction scheme. It is concluded that $La_2O_2CO_3$, which form by the interaction of La_2O_3 and CO_2, may decompose to produce CO or provide oxygen species which react with carbon accumulated on Ni crystallites due to CH_4 cracking to produce CO. The latter process is very fast over the Ni/La_2O_3 catalyst, as compared to carbon accumulation, and this imparts this catalyst its special stability characteristics.

1. INTRODUCTION

Synthesis gas plays an important role in the chemical industry since it is the feedstock material of many important industrial processes, such as methanol, ammonia, and Fischer–Tropsch synthesis. While steam reforming of methane (natural gas) is the established route of syngas production, the dry reforming with CO_2 may be an attractive alternative, especially for applications requiring synthesis gas with low H_2/CO ratio.

A major problem encountered with the process of CO_2 reforming of methane is rapid catalyst deactivation caused by excess carbon deposition, mainly through decomposition of the CO product, i.e., the Boudouard reaction, and/or methane cracking. Among the many materials which have been tested as potential catalysts for this reaction, supported noble metals (1–6) as well as Ni-based catalysts (7–21) have been found to exhibit promising catalytic performance.

Kroll *et al.* (7), have investigated the mechanism of carbon dioxide reforming of methane over Ni/SiO_2 catalyst. It was found that as soon as the catalyst is contacted with the reacting mixture, dehydrogenated carbon species, originating from the adsorption of methane and carbon dioxide, are deposited on the nickel particles. Under steady-state reaction conditions, a permanent pool of adspecies equivalent to one monolayer of carbide-like species is continuously fed by the dissociative activation of gaseous methane. This initial activation step of methane is shown to be reversible, since it allows a fast CH_4/CD_4 exchange, characterized by a marked isotopic effect.

Aparicio (11) has studied the kinetics of elementary surface reactions involved in the reforming of methane to synthesis gas over supported nickel, using isotopic methods. An overall model, that describes the reactions of methane with steam and CO_2 suggests that there is no single rate-determining step in methane reforming with either steam or CO_2 and that, under certain conditions, the availability of surface oxygen may play a key role in determining the rate. In fact, the step in which a C–O bond is formed is predicted to be slow, not because its rate constant is low, but because the coverage of OH drops quickly with temperature.

Ruckenstein and Hu (20, 21) studied the CO_2 reforming of methane over reduced NiO/MgO solid solution catalysts at 800°C. They found that two kinds of oxygen were formed over the catalysts during reaction, adsorbed oxygen which reacts rapidly with C species and lattice oxygen which reacts more slowly with C species. They concluded that a redox cycle of lattice oxygen formation through the oxidation of Ni and its reaction with C species takes place on the catalyst surface (20).

Studies conducted in this laboratory (12, 13) have shown that when Ni is appropriately supported onto a La_2O_3 carrier, it can exhibit good activity and excellent stability under conditions of dry reforming of methane, in contrast to other Ni-based catalysts, such as Ni/Al_2O_3, Ni/CaO, or Ni/Al_2O_3-CaO, which experience continuous deactivation with time-on-stream. This behavior has been attributed to the

0021-9517/99 $30.00

formation of a new type of surface structure on the Ni/La_2O_3 catalyst, which is resistant to deactivation by carbon deposition (12). This structure involves islands of $La_2O_2CO_3$ dispersed on the surface of Ni crystallites which interact with carbon deposited at their peripheral area producing CO and, simultaneously, liberating Ni sites for methane cracking (13, 14). $La_2O_2CO_3$ is produced by interaction of the La_2O_3 support with CO_2. This surface structure and surface chemistry imparts to the Ni/La_2O_3 catalyst its stability characteristics.

In the present study, the carbon and oxygen reaction pathways of the dry reforming of methane with CO_2 are investigated, as well as the origin of carbon accumulated over the Ni/La_2O_3 catalyst under reaction conditions. For this purpose, the technique of steady-state isotopic transient kinetic analysis (SSITKA) is applied as well as the use of isotopically labelled molecules in the reaction mixture.

2. EXPERIMENTAL

2.1. Catalyst Preparation and Characterization

Ni/La_2O_3, and Ni/γ-Al_2O_3 catalysts, containing 17 wt% Ni, were prepared by the wet-impregnation method, using nitrate salt ($Ni(NO_3)5H_2O$) as the metal precursor. Details of the preparation procedure have been reported previously (12, 13). The catalysts were characterized with respect to total and specific surface area and crystalline phases present before and after exposure to reaction conditions and details of the characterization procedures have been reported previously (12).

2.2. Transient Studies

Mass spectrometry. Chemical analysis of the gases during transients was done with an on-line mass spectrometer (Fisons, SXP Elite 300H or Sensorlab Quatrapole) equipped with a fast-response inlet capillary system. For the steady-state tracing experiments, 20 points/s could be recorded for a given peak (no scanning of the mass scale) using the electron multiplier detector. In the multiple peak data acquisition mode, 4 peaks/s could be followed with good signal-to-noise ratio. In certain exeriments, where the response of many species was recorded, the resolution was less than 4 peaks per s. Calibration of the mass spectrometer signal was performed based on prepared mixtures of known compositions. The output signal from the mass spectrometer detector was then converted to mole fraction, y (mol%), with appropriate software.

The steady-state isotopic tracing technique (SSITKA) was used in order to measure the concentration of the active reaction intermediate species. An extensive review of the steady-state isotopic tracing technique is given by Efstathiou and Verykios (22) and Schuurman and Mirodatos (23).

In the present SSITK experiments, the measurement of the responses of $^{13}CH_4$, $^{13}CO_2$, ^{13}CO, and $C^{18}O$, which allow quantification of active carbon-containing and oxygen-containing intermediate species in the reaction pathways from CH_4 and CO_2 to CO, was performed by recording the signals at $m/e = 17$, 45, 29, and 30, respectively. For the measurement of ^{13}CO ($m/e = 29$) in the presence of $^{13}CO_2$ ($m/e = 45$), the contribution of the $^{13}CO_2$ to the 29 peak was estimated by feeding to the mass spectrometer a mixture containing a given concentration of $^{13}CO_2$ in He. During this experiment, the settings in the ion source of the mass spectrometer were the same as those used in the real steady-state tracing experiments. Similar measurements were performed to estimate the ratio of 30/48 for the contribution of $C^{18}O_2$ ($m/e = 48$) to the $m/e = 30$ ($C^{18}O$). In other transient experiments, the gases H_2, CH_4, H_2O, $H_2{}^{18}O$, C_2H_6, $^{16}O^{18}O$, $^{18}O_2$, and $C^{16}O^{18}O$ were recorded at $m/e = 2$, 15, 18, 20, 30, 34, 36, and 46, respectively.

The reactor used in the present study consisted of two 4.0 mm i.d. sections of quartz tubes which serve as inlet and outlet to and from a quartz cell of 7.0 mm i.d. (nominal volume 2 ml). The entrance to the reactor cell was machined in such a way as to create local gas mixing. Heating was provided by a small furnace controlled by a programmable temperature controller. The temperature of the catalyst was measured by a K-type thermocouple placed within a quartz capillary well in the middle of the catalyst bed. The catalyst bed contained 5–10 mg catalyst diluted with an equal amount of low surface a-Al_2O_3. Due to the small length of the catalyst bed, the experiments performed are considered isothermal.

Isotopic mixtures. A mixture consisting of 20% $^{13}CH_4$, 20% CO_2, and 60% He was prepared using a lecture bottle of $^{13}CH_4$ which was of 99% ^{13}C content (Isotec Inc., USA). A mixture consisting of 20% CH_4, 15% CO_2, 5% $C^{18}O_2$, and 60% He was also prepared. To save isotope gas $C^{18}O_2$, and to reduce the contribution of $C^{18}O_2$ to the $C^{18}O$ signal due to cracking in the mass spectrometer, not all the 20% CO_2 in the ordinary mixture was replaced by $C^{18}O_2$ but only 5%. The $C^{18}O_2$ was of 96.3% ^{18}O purity (L'Air-Liquide, France). Similarly, the $CH_4/^{13}CO_2$/He mixture consists of 20% CH_4, 15% CO_2, 5% $^{13}CO_2$, and 60% He. The $^{13}CO_2$ was of 99% ^{13}C content (L'Air-Liquide, France). One percent Ar was also added to all isotopic mixtures (replacing 1% of He gas) to facilitate obtaining response curves of the gas not adsorbing or reacting with the catalyst. This response, when compared to the Ar response obtained upon bypassing the reactor, can be used to determine the holdup of gas in the reactor. All gas mixtures were used at the flow rate of 30 ml/min (ambient).

3. RESULTS AND DISCUSSION

3.1. Steady-State Tracing and Transient Isotopic Studies of Carbon-Containing Intermediate Species

The steady-state tracing technique, using isotopically labelled molecules such as $^{13}CH_4$, $^{13}CO_2$, and $C^{18}O_2$, and other transient methods have been applied in the present study to explore the mechanistic differences between Ni/La_2O_3 and Ni/Al_2O_3 catalysts under conditions of CO_2 reforming of methane. Ni/Al_2O_3 catalyst is considered to achieve a pseudo-steady-state performance as it is treated under the same conditions with Ni/La_2O_3 catalyst. CH_4 and CO_2 conversions over Ni/La_2O_3 and Ni/Al_2O_3 catalysts were the same under the conditions of the experiments presented in the following paragraphs.

Figure 1 shows the responses of ^{13}CO, $^{13}CH_4$, and Ar obtained 0.2 min before the last switch of the following sequence: $CH_4/CO_2/He$ (1 h) $\mapsto$ $^{13}CH_4/CO_2/He/Ar$ (10 min) $\mapsto$ $CH_4/CO_2/He$ (t) over the Ni/La_2O_3 catalyst at 750°C. The curve labelled "Ar" is the argon response, as the gas passes through the reactor containing the catalyst sample. The response of $^{13}CH_4$ reveals that reversibly adsorbed $^{13}CH_4$ exists on the catalyst surface, which was deposited during the 10-min $^{13}CH_4/CO_2/He$ treatment. This implies that during the reforming reaction over Ni/La_2O_3 catalyst, CH_4 is first adsorbed on the surface and then it cracks, leading to CH_x and eventually to carbon deposit. The area under the $^{13}CH_4$ curve in Fig. 1 can be used to estimate the quantity of reversibly adsorbed $^{13}CH_4$, following the calibration procedure which was described earlier. Thus, from Fig. 1 it can be estimated that 2.5 mol of reversibly adsorbed $^{13}CH_4$ exists on the catalyst surface per mol of surface Ni.

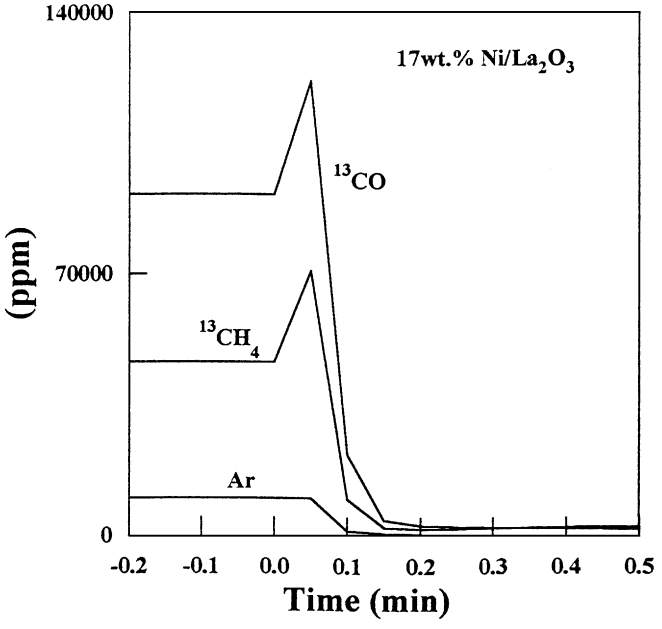

FIG. 1. Steady-state tracing of the reforming reaction of CH_4 with CO_2 at 750°C over the Ni/La_2O_3 catalyst. Gas delivery sequence: $CH_4/CO_2/He$ (750°C, 1 h) $\mapsto$ $^{13}CH_4/CO_2/He/Ar$ (750°C, 10 min) $\mapsto$ $CH_4/CO_2/He$ (750°C, t). The transient responses of Ar, ^{13}CO, and $^{13}CH_4$ are shown 0.2 min before the last switch was done.

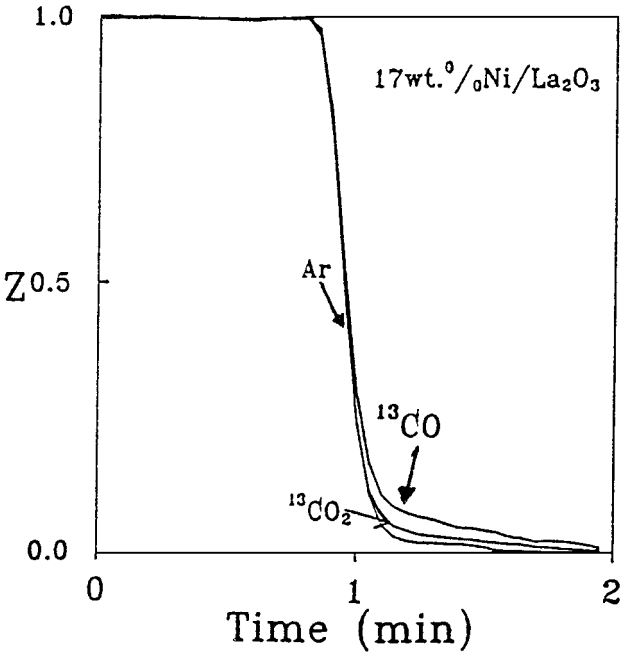

FIG. 2. Steady-state tracing of the reforming reaction of CH_4 with CO_2 at 750°C over the Ni/La_2O_3 catalyst. Gas delivery sequence: $CH_4/CO_2/He$ (750°C, 1 h) $\mapsto$ $CH_4/^{13}CO_2/He/Ar$ (750°C, 10 min) $\mapsto$ $CH_4/CO_2/He$ (750°C, t). The transient responses of Ar, ^{13}CO, and $^{13}CO_2$ are shown.

The ^{13}CO response which is also shown in Fig. 1 reflects the transient incorporation of ^{12}C into a ^{13}C-containing intermediate species pool, and the depletion of the latter with time-on-stream. The area corresponding to the ^{13}CO response curve is proportional to the amount of active carbon-containing intermediate species, which are in the carbon-pathway to form CO, originating from the CH_4 molecule. This amount corresponds to 1.2 mol ^{13}CO/mol Ni. Thus, a fairly large quantity of carbon-containing species, originating from the methane molecule, exist on the catalyst surface. Under the conditions of the present experiment, the CH_4 conversion was 70%. Similar experiments at low CH_4 conversions do not allow an accurate measurement of active carbon.

In order to trace the reaction pathway of carbon derived from the CO_2 molecule, a steady-state tracing experiment, similar to that presented in Fig. 1, was conducted over Ni/La_2O_3 at 750°C, this time labelling the feed with $^{13}CO_2$. The following switching sequence was used: $CH_4/CO_2/He$ (1 h) $\mapsto$ $CH_4/^{13}CO_2/He/Ar$ (10 min) $\mapsto$ $CH_4/CO_2/He$ (t). Figure 2 shows the ^{13}CO, $^{13}CO_2$, and Ar responses of the reactor output composition. The results are expressed in terms of the variable Z, which represents the fraction of

the ultimate change (giving $Z = 1$) as a function of time. Thus Z is defined by $Z(t) = (y(t) - y_\infty)/(y_0 - y_\infty)$, where the subscripts 0 and ∞ refer to values of y (mole fraction) just before the switch ($t = 0$) and long after the switch ($t \to \infty$). For the curve labelled $^{13}CO_2$, y represents the mole fraction of $^{13}CO_2$ in the gas phase at the reactor outlet. Thus if there was no reversibly adsorbed $^{13}CO_2$ under $^{12}CH_4/^{13}CO_2$/He treatment, then the $^{13}CO_2$ response would have been identical to the Ar response curve. In the case shown in Fig. 2, the $^{13}CO_2$ response is somewhat delayed as compared with the Ar response. This leads to the suggestion that there is a small quantity of reversibly adsorbed CO_2, corresponding to an amount of 0.15 mol $^{13}CO_2$/mol Ni. It should be pointed out that the fact that the quantities of adsorbed species are estimated on a per mol of surface Ni basis does not necessarily imply that such species reside on the Ni surface alone. The decay of the ^{13}CO response curve represents the depletion of the ^{13}C-containing intermediate species pool. The area difference between the ^{13}CO and Ar curves is proportional to the amount of active carbon-containing intermediate species, which are in the carbon-pathway to form CO from the CO_2 molecule. This amount is found to be 0.45 mol ^{13}CO/mol Ni, which is less than the active carbon-containing intermediate species which are in the carbon-pathway to form CO from the CH_4 molecule (1.2 mol CO/mol Ni). This tendency is in line with the fact that the majority of carbon formation is due to cracking of the CH_4 molecule as is illustrated below. The smaller quantity of reversibly adsorbed CO_2 as compared with that of reversibly adsorbed CH_4 during CH_4/CO_2/He reaction over Ni/La_2O_3 catalyst is in agreement with the stronger CO_2 adsorption as compared with that of CH_4 adsorption over Ni/La_2O_3 catalyst, which has been confirmed by kinetic experiments (24). This means that a large quantity of CO_2 is irreversibly adsorbed.

The steady-state tracing technique applied in the present work provides the amount of active carbon-containing species which participate in the reaction pathway towards CO formation, under conditions of methane reforming with CO_2. Obviously, these amounts are sensitive to the degree of conversion of the reactant molecules. In the present study, consistently high overall conversions were employed, approximately 70% for CH_4 and 80% for CO_2. Thus, the results reported should be considered to reflect the strong influence of a distribution of partial pressures of reactants and products, developed along the length of the catalyst bed, on surface coverages of intermediate species.

Steady-state tracing experiments using isotopic mixtures have also been conducted over the Ni/Al_2O_3 catalyst. Figure 3 shows the Ar, ^{13}CO, and $^{13}CH_4$ responses during the last switch of the following sequence: CH_4/CO_2/He (750°C, 1 h) → $^{13}CH_4/CO_2$/He/Ar (750°C, 10 min) → CH_4/CO_2/He (750°C, t). As is shown, there is a small quantity of reversibly adsorbed CH_4 during the reforming reaction

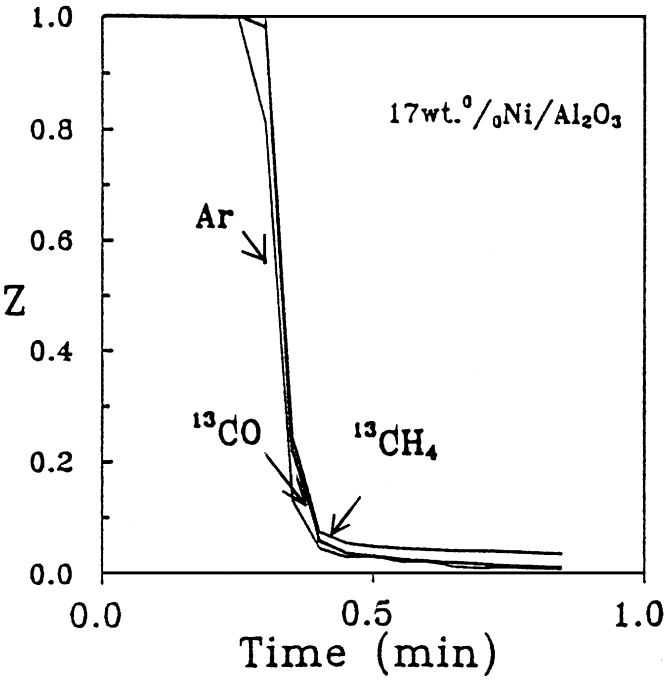

FIG. 3. Steady-state tracing of the reforming reaction of CH_4 with CO_2 at 750°C over the Ni/Al_2O_3 catalyst. Gas delivery sequence: CH_4/CO_2/He (750°C, 1 h) ↦ $^{13}CH_4/CO_2$/He/Ar (750°C, 10 min) ↦ CH_4/CO_2/He (750°C, t). The transient responses of Ar, ^{13}CO, and $^{13}CH_4$ are shown.

over the Ni/Al_2O_3 catalyst. The area difference between Ar and $^{13}CH_4$ response curves corresponds to an amount of 0.25 mol CH_4/mol Ni, a quantity which is significantly less than the corresponding one over the Ni/La_2O_3 catalyst. The decay of the ^{13}CO response curve represents the depletion of ^{13}C-containing intermediate species pool. The area difference between the ^{13}CO and the Ar curves corresponds to an equivalent amount of 0.78 mol C/mol Ni, a quantity less than the one corresponding to the Ni/La_2O_3 catalyst. It is evident that the quantity of the carbon-containing intermediate species in the carbon-pathway to form CO from the CH_4 molecule is much higher in the case of the Ni/La_2O_3 than in the case of the Ni/Al_2O_3 catalyst.

A steady-state isotopic tracing experiment was also performed to investigate the CO_2 molecular pathway over the Ni/Al_2O_3 catalyst. Figure 4 presents the responses of Ar, ^{13}CO, and $^{13}CO_2$ during the last switch of the following sequence: CH_4/CO_2/He (750°C, 1 h) ↦ $CH_4/^{13}CO_2$/He/Ar (750°C, 10 min) ↦ CH_4/CO_2/He (750°C, t). As is shown, there is reversibly adsorbed CO_2 which corresponds to a quantity of 0.35 mol C/mol Ni, while the active-carbon-containing species derived from the CO_2 molecule, which are presented by the ^{13}CO curve, correspond to a quantity of 0.9 mol C/mol Ni. This result shows that the quantity of intermediate active carbon species formed through the CO_2 molecule and the reversibly adsorbed CO_2 onto Ni/Al_2O_3 is higher than the respective value derived from the CH_4

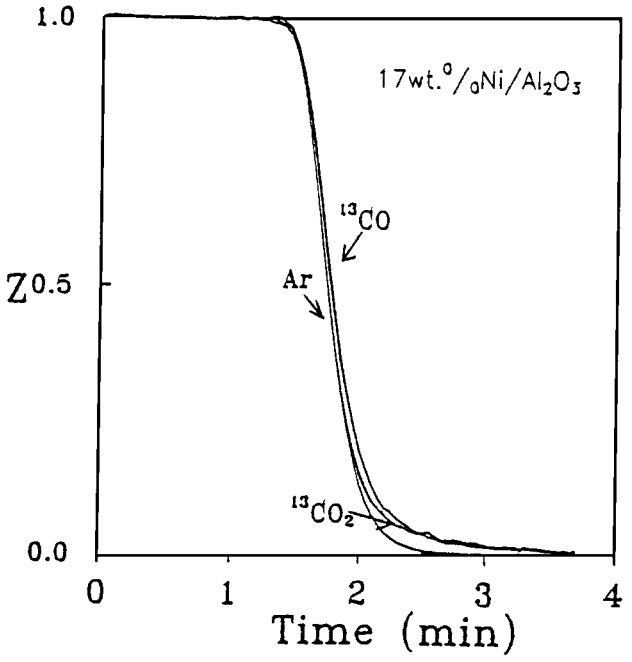

FIG. 4. Steady-state tracing of the reforming reaction of CH_4 with CO_2 at 750°C over the Ni/Al_2O_3 catalyst. Gas delivery sequence: CH_4/CO_2/He (750°C, 1 h) ↦ $CH_4/^{13}CO_2$/He/Ar (750°C, 10 min) ↦ CH_4/CO_2/He (750°C, *t*). The transient responses of Ar, ^{13}CO, and $^{13}CO_2$ are shown.

molecule. In order to compare the results derived from the SSITK analysis conducted over Ni/La_2O_3 and Ni/Al_2O_3 catalysts, the respective values of reversibly adsorbed CH_4 and CO_2, as well as the quantities of the active intermediate carbon-containing species, are summarized in Table 1.

Comparison of the amount of active carbon-containing species formed over Ni/La_2O_3 and Ni/Al_2O_3 catalysts, derived from the methane molecule, reveals that this quantity is higher in the case of Ni/La_2O_3 than in the case of Ni/Al_2O_3 catalysts. The opposite tendency is observed concerning the amount of active carbon-containing intermediate species derived from the CO_2 molecule. From this observation it may be concluded that the relative rates of the reaction steps of CO formation from the CH_4 or the CO_2 molecules are influenced by the carrier of the Ni crystallites or that different mechanistic routes are followed. It may be concluded that the reaction steps of the CH_4 reaction pathway to form CO are faster while those of CO_2 are slower in the case of Ni/Al_2O_3 than in the case of Ni/La_2O_3 catalysts. This conclusion is also supported by the fact that the reversibly adsorbed CH_4 onto the Ni/La_2O_3 catalyst is nearly one order of magnitude higher than that onto the Ni/Al_2O_3 catalyst. In turn, this observation may imply an interaction between CH_4 and the La_2O_3 support or, more probably, with $La_2O_2CO_3$ which form by interaction of La_2O_3 with CO_2 and which also exist, in island form, on the surface of the large nickel crystallites.

TABLE 1

Quantities of Reversibly Adsorbed CH_4 and CO_2, and Active Intermediate Carbon-Containing Species Derived from the CH_4 or CO_2 Molecular Pathways over Ni/La_2O_3 and Ni/Al_2O_3 Catalysts, in molC per mol of Surface Ni

	Ni/La_2O_3	Ni/Al_2O_3
Reversibly adsorbed CH_4	2.53	0.25
Active carbon from CH_4	1.2	0.78
Reversibly adsorbed CO_2	0.15	0.35
Active carbon from CO_2	0.45	0.9

Note. The reproducibility of these measurments is in the range ±5–10%.

The observation of reversibly adsorbed CH_4, as well as active carbon species derived from CH_4, which lead to CO production, suggests that the dissociation of CH_4 into CH_x species and oxidation of these species to form CO is a slow step over the Ni/La_2O_3 catalyst. The fact that the respective amount of reversibly adsorbed CO_2 and active carbon species derived from the CO_2 molecule are considerably smaller than those corresponding to CH_4 leads to the suggestion that the interaction of CO_2 with the catalytic surface is a fast step, compared to that of the CH_4 molecule. Considering the fact that methane activation occurs on Ni crystallites while CO_2 preferably reacts with La_2O_3 (12, 13), the following reaction steps may be considered to describe the interaction of the reactant molecules with the catalyst surface:

$$CH_4 + Ni \rightarrow Ni\cdots CH_4 \rightarrow NiC + 2H_2 \quad \text{slow} \quad [1]$$

$$CO_2 + La_2O_3 \rightleftharpoons La_2O_2CO_3 \quad \text{fast.} \quad [2]$$

The dissociation of adsorbed methane is slow while the reaction between CO_2 and La_2O_3 is fast.

These results may be related to a kinetic isotope effect study conducted over the Ni/La_2O_3 catalyst by replacing CH_4 with CD_4 in the feed stream under reforming conditions (12). A reduction in the rate of CO formation by a factor of 1.19 to 1.97 was observed upon switching the feed from CH_4/CO_2 to CD_4/CO_2. This result also indicates that methane activation over the Ni/La_2O_3 catalyst is a slow step. Similarly, the smaller amount of active carbon-containing species derived from CH_4 which was observed over the Ni/Al_2O_3 catalyst is related to the negligible reduction in the rate of CO formation, by a factor of 1.02 to 1.08, which was observed upon switching CH_4/CO_2 to CD_4/CO_2, suggesting that methane activation over the Ni/Al_2O_3 catalyst is a fast step. The results of both studies indicate either that different mechanisms are followed over the two catalysts, or that the relative rates of surface transformation steps are significantly affected by the carrier of the Ni crystallites, as has been discussed in previous communications (12–14).

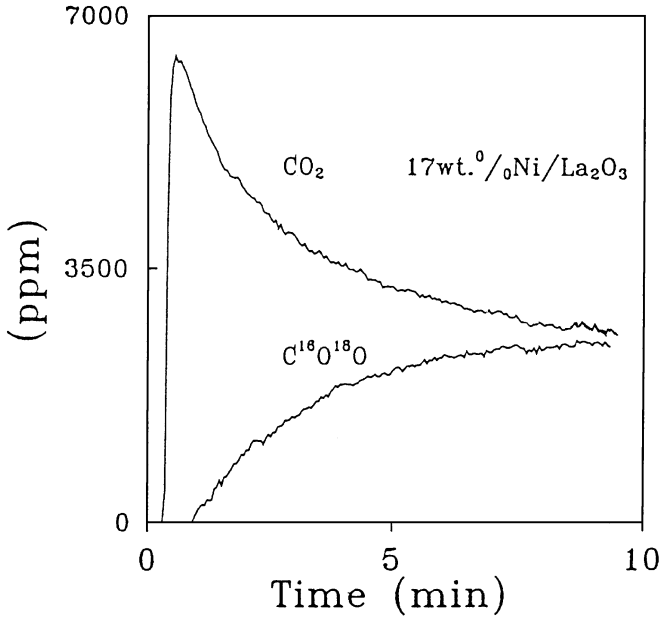

FIG. 5. Transient CO_2 and $C^{16}O^{18}O$ responses obtained during exposure of the reduced Ni/La_2O_3 catalyst to 1%$C^{18}O_2$/He mixture at 750°C.

3.2. Steady-State Tracing and Transient Isotopic Studies of Oxygen-Containing Intermediate Species

In order to investigate the oxygen pathway of the CH_4 reforming reaction with CO_2 over the Ni/La_2O_3 catalyst, the following experiment was conducted: The Ni/La_2O_3 catalyst was reduced in H_2 flow at 750°C for 2 h and then was purged with He for 5 min. Following this treatment, the feed was switched to 1% $C^{18}O_2$/He mixture, and the responses of CO_2 and $C^{16}O^{18}O$ were monitored. Figure 5 presents the production of $C^{16}O^{18}O$ and CO_2 during the titration of the Ni/La_2O_3 catalyst with $C^{18}O_2$ at 750°C. It is obvious that the only pool of ^{16}O is the La_2O_3 support, so the production of $C^{16}O^{18}O$ and $C^{16}O_2$ is the result of the exchange of ^{18}O from $C^{18}O_2$ in the gas phase with the lattice ^{16}O of the La_2O_3 support. It is also worth noticing that there is a large production of $C^{16}O_2$. This is the result of the oxidation of carbon deposited on the catalyst surface due to the $C^{18}O_2$ dissociation, by ^{16}O atoms originating from the La_2O_3 support. The $C^{16}O_2$ response decreases after going through a maximum, due to the depletion of the ^{16}O pool of the La_2O_3 support. This experiment clearly indicates that there is a large dynamic oxygen pool on the Ni/La_2O_3 catalyst participating in the reaction.

To investigate the oxygen reservoir on the catalyst surface, which participates in the production of CO, a steady-state tracing experiment using $C^{18}O_2$ in the feed stream, was also conducted. Thus, the following sequence was applied: CH_4/CO_2/He (750°C, 1 h) ↦ $CH_4/C^{18}O_2$/He (750°C, 10 min) ↦ CH_4/CO_2/He (750°C, *t*). The composition of the isotopic mixture was 20% CH_4/5% $C^{18}O_2$/15% CO_2/59% He/1% Ar. The responses of Ar, $C^{18}O$, $C^{16}O^{18}O$, and $C^{18}O_2$ obtained during the last switch are presented in Fig. 6. It is shown that there is a large quantity of $C^{18}O$ and $C^{16}O^{18}O$ produced, and a smaller quantity of $C^{18}O_2$. The responses of the $C^{18}O$ and $C^{16}O^{18}O$ remain constant for approximately 0.3 min after the switch of the feed from $CH_4/C^{18}O_2$/Ar/He to CH_4/CO_2/He, and they go through a maximum during 1 min on stream in the CH_4/CO_2/He mixture. The transient responses of gaseous species containing ^{18}O, shown in Fig. 6, clearly suggest that during the 10-min treatment of the Ni/La_2O_3 catalyst at 750°C with $CH_4/C^{18}O_2$/He/Ar, a large reservoir of ^{18}O species is formed, which subsequently is depleted under CH_4/CO_2/He treatment, through reactions [3]–[5], leading to $C^{18}O$, $C^{16}O^{18}O$, and $C^{18}O_2$,

$$La_2O_3 + C^{18}O_2 \rightleftharpoons La_2O_2C^{18}O_2O \quad [3]$$

$$La_2O_2C^{18}O_2O + C(s) \rightarrow La_2O_3 + 2C^{18}O \quad [4]$$

$$CO_2 + La_2O_2C^{18}O_2O \rightleftharpoons C^{18}O_2 + La_2O_2CO_3. \quad [5]$$

A small quantity of $H_2{}^{18}O$ was also produced during this experiment. The quantity of oxygen species accumulated on the catalyst surface during $CH_4/C^{18}O_2$/He treatment corresponds to 130 monolayers of ^{18}O (based on 1% dispersion of Ni/La_2O_3 catalyst). This number corresponds to 3750 μmol ^{18}O/g La_2O_3. Obviously, this quantity cannot reside on the Ni surface but must be primarily on La_2O_3 or on compounds formed by the interaction of carbon dioxide with lanthana, such as $La_2O_2CO_3$.

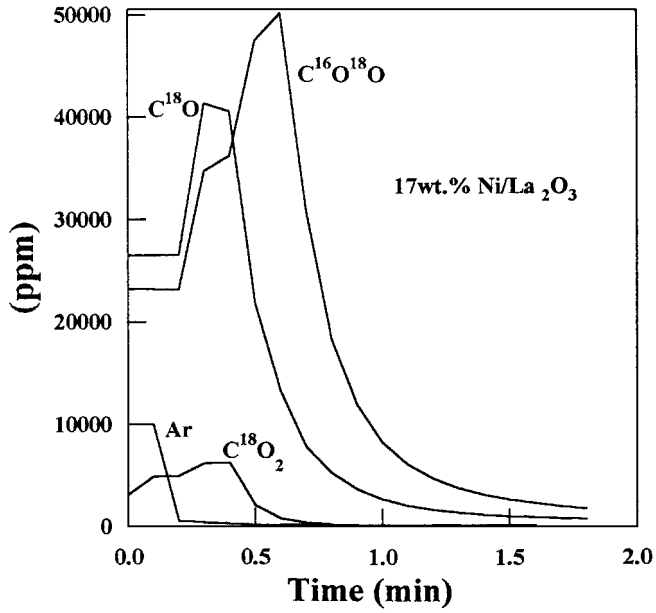

FIG. 6. Steady-state tracing of the reforming reaction of CH_4 with CO_2 at 750°C over the Ni/La_2O_3 catalyst. Gas delivery sequence: CH_4/CO_2/He (750°C, 1 h) ↦ $CH_4/C^{18}O_2$/He/Ar (750°C, 10 min) ↦ CH_4/CO_2/He (750°C, *t*). The transient responses of Ar, $C^{18}O$, $C^{18}O_2$, and $C^{16}O^{18}O$ are shown.

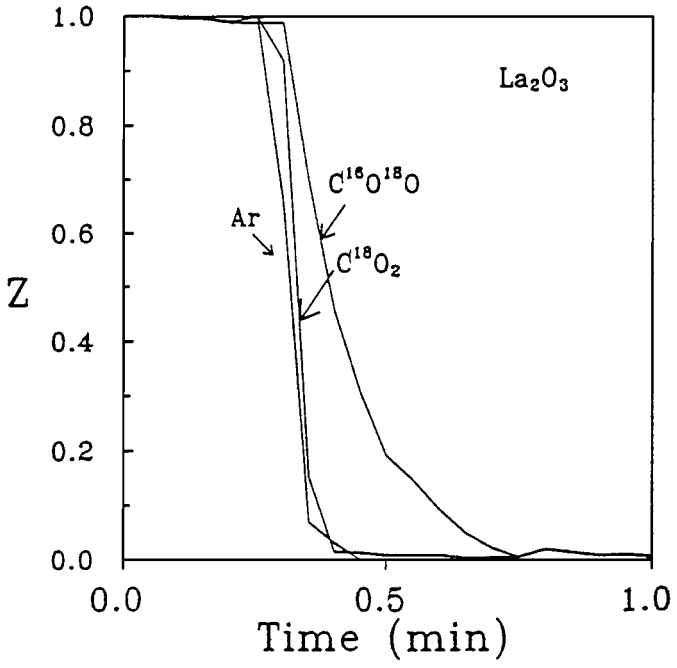

FIG. 7. Steady-state tracing of the reforming reaction of CH_4 with CO_2 at 750°C over the La_2O_3 support. Gas delivery sequence: CH_4/CO_2/He (750°C, 1 h) ↦ $CH_4/C^{18}O_2$/He/Ar (750°C, 10 min) ↦ CH_4/CO_2/He (750°C, *t*). The transient responses of $C^{18}O_2$ and $C^{16}O^{18}O$ are shown.

To further explore this view, the same-steady state tracing experiment was performed over the La_2O_3 support alone, using a mixture of 20% CH_4/2% $C^{18}O_2$/18% CO_2/59% He/1% Ar. The response of Ar, $C^{16}O^{18}O$, and $C^{18}O_2$ were followed during the last switch of the following sequence: CH_4/CO_2/He (750°C, 1 h) ↦ $CH_4/C^{18}O_2$/He/Ar (750°C, 10 min) ↦ CH_4/CO_2/He (750°C, *t*). The results presented in Fig. 7, demonstrate that there is reversibly adsorbed $C^{18}O_2$ and a higher quantity of reversibly adsorbed $C^{16}O^{18}O$. The quantity of $C^{18}O_2$ is smaller than the quantity of $C^{16}O^{18}O$ because at these experimental conditions, the mixture contains $C^{16}O_2$ and, therefore, $C^{16}O^{18}O$ is more easily produced than $C^{18}O_2$. Thus, during the 10-min treatment of the La_2O_3 support at 750°C with the $CH_4/C^{18}O_2$/He/Ar mixture, a large reservoir of ^{18}O species is formed, corresponding to 961 μmol ^{18}O/g La_2O_3.

A comparison between the 3750 μmol $^{18}O/gLa_2O_3$ over Ni/La_2O_3 catalyst and the 961 μmol $^{18}O/gLa_2O_3$ over La_2O_3 support clearly shows that in the first case the quantity of adsorbed ^{18}O is four times greater than in the second one. Apparently, Ni has a very significant effect on the oxygen adsorption on the La_2O_3 support under reaction conditions. It can be suggested that Ni weakens the bond among La and O atoms due to electronic interactions. Thus, oxygen atoms from La_2O_3 support are more easily exchanged with oxygen atoms from the gas phase. To investigate the CO_2 reaction pathway over the Ni/La_2O_3 catalyst, the following experiment was conducted: The reduced catalyst was first exposed to $CH_4/^{13}CO_2$/He for 10 min at 750°C and then the feed was switched to $CH_4/C^{18}O_2$/He. During the last switch, in addition to the production of $C^{18}O$ and $C^{16}O^{18}O$, the responses of ^{13}CO and $^{13}C^{18}O$ were also of interest. The responses of $C^{18}O$ and $C^{16}O^{18}O$ are shown in Fig. 8a, while

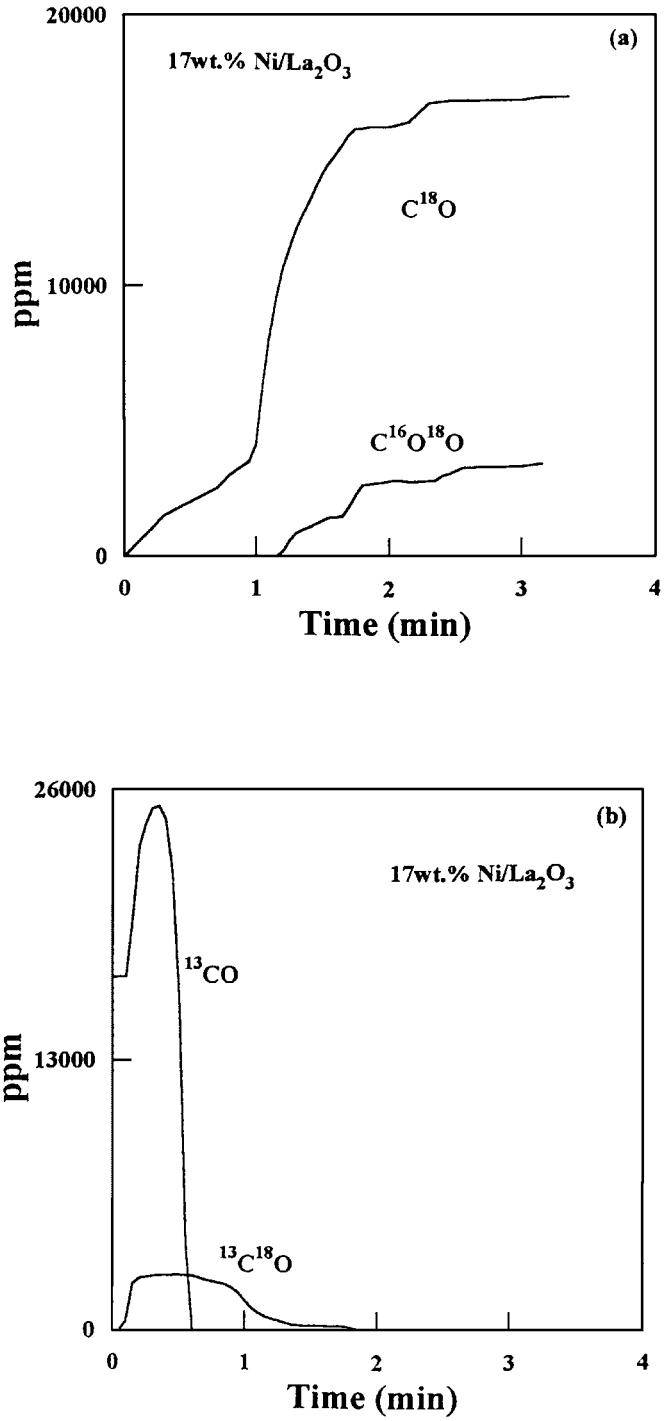

FIG. 8. Transient responses of $C^{18}O$ and $C^{16}O^{18}O$ (a) and ^{13}CO and $^{13}C^{18}O$ (b) obtained over the Ni/La_2O_3 catalyst during the switch: $CH_4/^{13}CO_2$/He (10 min) ↦ $CH_4/C^{18}O_2$/He (*t*) at 750°C.

responses of ^{13}CO and $^{13}C^{18}O$ are presented in Fig. 8b. In Fig. 8a it is interesting to note the time delay of appearance of the $C^{16}O^{18}O$ product, due to the exchange of lattice ^{16}O of La_2O_3 with ^{18}O of the gas phase. As is demonstrated in Fig. 8b, as the pool of ^{13}C and $^{13}C^{18}O$ is depleted, the signals of ^{13}CO and $^{13}C^{18}O$ decrease after passing through a maximum value. Accounting for the fact that during dry reforming of CH_4 over Ni/La_2O_3 the CO_2 molecule interacts with the carrier to form the $La_2O_2CO_3$ species (12), the following reaction scheme can be proposed to take place on the carrier surface.

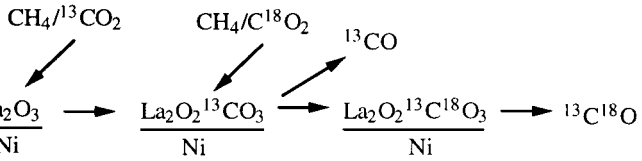

It can be pointed out that the C in the $La_2O_2CO_3$ species, which originates from gas-phase CO_2, reacts with O atoms from the gas phase or that $La_2O_2CO_3$ decompose to produce CO and oxygen species. The decomposition of $La_2O_2CO_3$ may be expressed by the equations

$$La_2O_2CO_3 + H(s) \rightarrow La_2O_3 + CO + OH^- \quad [6]$$

$$OH^- + C(s) \rightarrow CO + H(s) \quad [7]$$

$$La_2O_2CO_3 + C(s) \rightarrow La_2O_3 + 2CO. \quad [8]$$

These equations show that the decomposition of the $La_2O_2CO_3$ species is promoted by H(s) species derived from CH_4 decomposition. As has been shown elsewhere (12, 13), these oxygen species react with carbon deposited on Ni crystallites to form CO, thus cleaning the Ni surface of carbon deposits and imparting to the catalyst its excellent stability characteristics.

A steady-state tracing experiment using the 20% CH_4/2% $C^{18}O_2$/18% CO_2/59% He/1% Ar isotopic mixture, was also conducted over the Ni/Al_2O_3 catalyst in order to investigate the oxygen pathway during CH_4 reforming at 750°C. The following sequence was applied: $CH_4/CO_2/He$ (1 h) → $CH_4/C^{18}O_2$/He/Ar (10 min) → CH_4/CO_2/He (*t*). During the last switch no production of $C^{16}O^{18}O$ was detected, indicating that there is no detectable exchange of lattice oxygen atoms with oxygen in the gas phase.

The steady-state tracing experiments reported above allow the investigation of the oxygen reaction pathway, from the CO_2 molecule, and support the notion of the formation of the $La_2O_2CO_3$ species, which has been reported in previous study (12, 13). Figure 7 clearly demonstrates that there is a large affinity for interaction and oxygen exchange between La_2O_3 and CO_2. Furthermore, Fig. 8 clearly shows that the production of $C^{18}O$, $C^{16}O^{18}O$, and $C^{18}O_2$ is due to the depletion of the reservoir of ^{18}O species existing on the La_2O_3 support, which were formed during exposure of the Ni/La_2O_3 catalyst to the $CH_4/C^{18}O_2$/He mixture for 10 min. Thus, the existence of a large dynamic oxygen pool, which participates in the formation of CO under reforming conditions, over the Ni/La_2O_3 catalyst, in comparison with the absence of a similar oxygen pool on the Ni/Al_2O_3 catalyst, supports the suggestion that the removal of carbon species by oxygen atoms of the $La_2O_2CO_3$ species is responsible for the high degree of stability of the Ni/La_2O_3 catalyst. It may also be reasoned that the interaction of the carbon species with the oxycarbonates is a fast step under the present reaction conditions.

3.3. Origin of the Carbon Species Accumulated on the Catalyst During Reaction

To investigate the origin of carbon species formed under reaction conditions over the Ni/La_2O_3 catalyst, the following experiment was conducted: The catalyst was first treated with $^{13}CH_4/CO_2$/He (20/20/60 vol%) mixture for 0.5 h at 750°C, followed by a 3-min He purge. The feed was then switched to 10% O_2/He mixture in order to carry out isothermal oxidation of the carbon species accumated on the catalyst surface during reaction.

Figure 9a shows the $^{12}CO_2$, ^{12}CO, and $^{13}CO_2$ responses obtained during the isothermal oxidation. The $^{12}CO_2$ and ^{12}CO responses are due to the oxidation of carbon deposits derived from the CO_2 molecule, while the $^{13}CO_2$ response is due to the oxidation of carbon species derived from the $^{13}CH_4$ molecule during reforming reaction. It is worth noticing that oxidation of the carbon derived from the CH_4 molecule does not lead to CO production (no ^{13}CO was detected).

It has been observed that the carbon formed on the Ni/La_2O_3 catalyst during dry reforming is more reactive towards hydrogenation than oxidation. For this reason, the isothermal oxidation of carbon species, which was described in Fig. 9a, was followed by isothermal hydrogenation after purging the reactor with He for 10 min. Figure 9b shows the $^{13}CH_4$ and $^{12}CH_4$ responses obtained during the isothermal hydrogenation. These two experiments together show that most of the carbon accumulated over the Ni/La_2O_3 catalyst is derived from the reaction pathway of CH_4 rather than from the CO_2 molecule. In fact, approximately 80% of carbon accumulated originates from CH_4 cracking.

In contrast to this observation, the investigation of the origin of carbon during reforming reaction over Ni/Al_2O_3 catalyst has shown that the majority of the carbon accumulated comes from dissociation of the CO_2 molecule. This result derives from the isothermal oxidation of carbon species formed after 30 min reaction with $^{13}CH_4/CO_2$/He mixture at 750°C. The ^{12}CO, $^{12}CO_2$, and $^{13}CO_2$ responses were recorded during the previous oxidation experiment. It is interesting to mention that the carbon derived from $^{13}CH_4$ cracking is oxidized directly to $^{13}CO_2$ while no ^{13}CO is produced. In contrast, the carbon derived from CO_2 dissociation, is oxidized to CO as well. The majority of carbon,

approximately 85%, derives from the dissociation of CO_2, while only 15% of accumulated carbon derives from cracking of CH_4. Isothermal hydrogenation experiment, after the isothermal oxidation of carbon species, has shown that a negligible quantity of carbon remains on the catalyst surface after the oxidation step. The quantities of $^{13}CH_4$, CH_4, CO_2, $^{13}CO_2$, CO, and ^{13}CO obtained during isothermal oxidation followed by isothermal hydrogenation at 750°C of carbon species formed over Ni/La_2O_3 and Ni/A_2O_3 catalysts after their exposure to the isotopic mixture $^{13}CH_4/CO_2/He$ for 0.5 h are shown in Table 2. The reproducibility of the data is in the range ±5–10%.

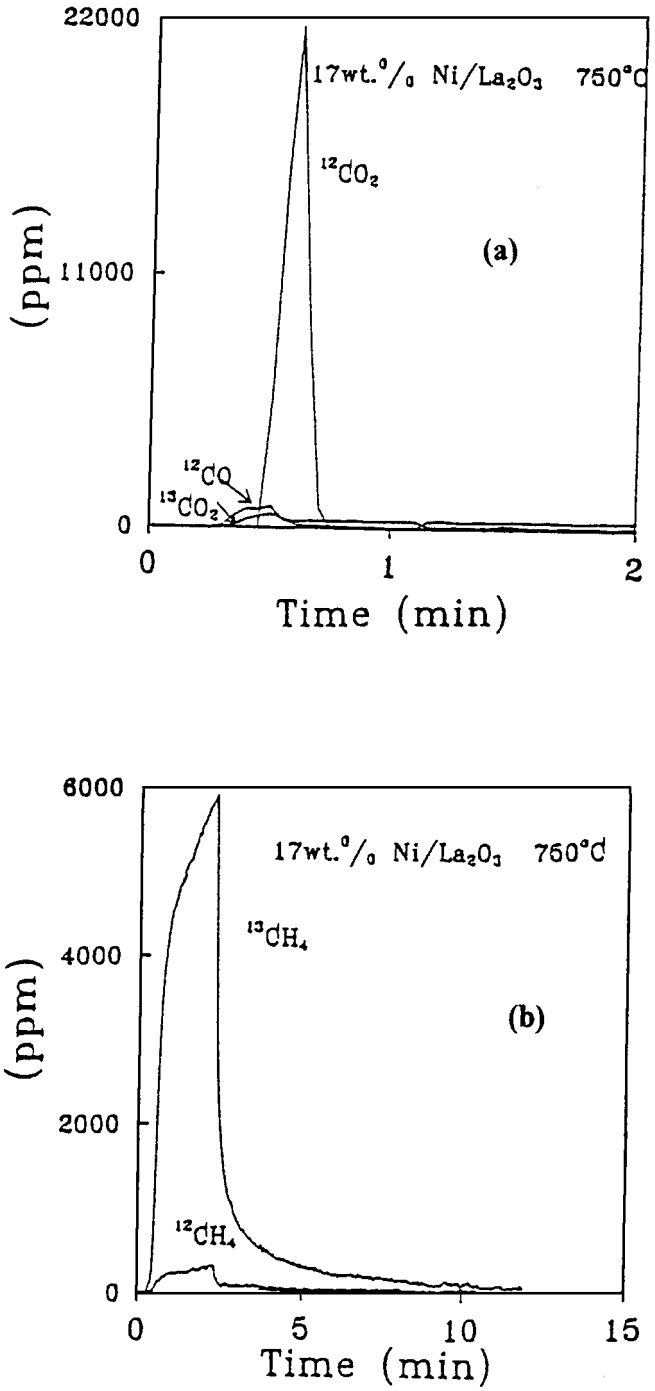

FIG. 9. (a) Isothermal oxidation of carbon species formed after 30 min reaction with the $^{13}CH_4/CO_2/He$ mixture at 750°C over Ni/La_2O_3 catalyst. (b) Isothermal hydrogenation of the remaining carbon species following the isothermal oxidation.

TABLE 2

Quantities of CO, ^{13}CO, CO_2, $^{13}CO_2$, CH_4, and $^{13}CH_4$ Obtained during Isothermal Oxidation Followed by Isothermal Hydrogenation at 750°C of Carbon Species Formed over Ni/La_2O_3 and Ni/Al_2O_3 Catalysts, in molC per mol of Surface Ni, after Their Exposure to the Isotopic Mixture $^{13}CH_4/CO_2/He$ for 0.5 h

	Ni/La_2O_3	Ni/Al_2O_3
$^{13}CH_4$	3.14	0
CH_4	0.21	0
CO_2	0.7	7.25
$^{13}CO_2$	0.08	1.43
CO	0.15	0.83
^{13}CO	0	0

Note. The reproducibility of this data is in the range ±5–10%.

CONCLUSIONS

The following conclusions may be derived from the results of the present study:

(1) The detection of reversibly adsorbed CH_4 under reaction conditions indicates that the activation of CH_4 may be considered a slow step over the Ni/La_2O_3 catalyst.

(2) The quantity of active carbon-containing intermediate species which lead to the formation of CO and derive from the CH_4 molecular route is significantly higher than the respective amount derived from CO_2 dissociation over Ni/La_2O_3 catalyst.

(3) The dissociation of the CO_2 molecule over Ni/La_2O_3 catalyst is a fast step in comparison to CH_4 activation. The opposite tendency is followed over the Ni/Al_2O_3 catalyst.

(4) The steady-state tracing results obtained over the Ni/Al_2O_3 catalyst suggest that the reaction steps of the CH_4 molecular route to form CO are faster than those observed over the Ni/La_2O_3 catalyst,while the opposite trend is observed for the CO_2 molecular pathway.

(5) The La_2O_3 support behaves as a dynamic oxygen pool under reforming reaction conditions over Ni/La_2O_3 catalyst. The oxidation of carbon species to form CO by oxygen originating from the oxycarbonates is a fast step in the reaction sequence.

(6) $La_2O_2CO_3$ species were found to decompose to CO product under steady-state reaction conditions over the Ni/La_2O_3 catalyst.

(7) Ni promotes oxygen adsorption on the La_2O_3 support.

REFERENCES

1. Richardson, J. T., and Paripatyadar, S. A., *Appl. Catal.* **61**, 293 (1990).
2. Rostrup-Niesen, J. R., and Bak Hansen, J. H., *J. Catal.* **38**, 144 (1993).
3. Tsipouriari, V. A., Efstathiou, A. M., Zhang, Z. L., and Verykios, X. E., *Catal. Today* **21**, 579 (1994).
4. Keulen, A. N. J., Seshan, K., Hoebink, J. H. B., and Ross, J. R. H., *J. Catal.* **166**, 306 (1997).
5. Stagg, S. M., Romeo, E., Padro, C., and Resasco, D. E., *J. Catal.* **178**, 137 (1998).
6. Bradford, M. C. J., and Vannice, M. A., *J. Catal.* **173**, 157 (1998).
7. Kroll, V. C. H., Swaan, H. M., Lancombe, S., and Mirodatos, C., *J. Catal.* **164**, 387 (1997).
8. Gadalla, A. M., and Sommer, M. E., *Chem. Eng. Sci.* **44**, 2825 (1989).
9. Gadalla, A. M., and Bower, B., *Chem. Eng. Sci.* **43**, 3049 (1988).
10. Kim, G. L., Cho, D. S., Kim, K., and Kim, J. H., *Catal. Lett.* **28**, 41 (1994).
11. Aparicio, L. M., *J. Catal.* **165**, 262 (1997).
12. Zhang, Z. L., and Verykios, X. E., *Appl. Catal.* **138**, 109 (1996); Zang, Z. L., and Verykios, X. E., *Catal. Lett.* **38**, 175 (1996).
13. Zhang, Z. L., Verykios, X. E., Mac Donald, S. M., and Affrossman, S., *J. Phys. Chem.* **100**, 744 (1996).
14. Slagtern, A., Schuurman, Y., Leclercq, C., Verykios, X., and Mirodatos, C., *J. Catal.* **172**, 118 (1997).
15. Lemonidou, A. A., Goula, M. A., and Vasalos, I. A., *Catal. Today* **46**, 175 (1998).
16. Choi, J., Moon, K., Kim, Y. G., Lee, J. S., Kim, G. H., and Trimm, D. L., *Catal. Lett.* **52**, 43 (1998).
17. Chen, Y., Tomishige, K., and Fujimoto, K., *Appl. Catal.* **161**, 11 (1997).
18. Tomishige, K., Chen, Y., and Fujimoto, K., *J. Catal.* **181**, 91 (1999).
19. Wang, S., and Lu, G. Q., *Appl. Catal.* **169**, 271 (1998).
20. Hu, Y. H., and Ruckenstein, E., *Catal. Lett.* **36**, 145 (1996).
21. Ruckenstein, E., and Hu, Y. H., *Catal. Lett.* **51**, 183 (1998).
22. Efstathiou, M. A., and Verykios, X. E., *Appl. Catal.* **151**, 109 (1997).
23. Schuurman, Y., and Mirodatos, C., *Appl. Catal.* **151**, 305 (1997).
24. Tsipouriari, V. A., and Verykios, X. E., in preparation.